Guaranteed State Estimation via Direct Polytopic Set Computation for Nonlinear Discrete-Time Systems

Mohammad Khajenejad, *Member, IEEE*, Fatima Shoaib, and Sze Zheng Yong, *Member, IEEE*

***Abstract*—This letter introduces a set-theoretic state estimation approach for bounded-error nonlinear discrete-time systems, subject to nonlinear observations or constraints, when polytope-valued uncertainties are assumed. Our approach relies on finding a polytopic enclosure to the true range of nonlinear mappings via the direct use of hyperplane and vertex representations of polytopes. In particular, we derive a tractable enclosure of the set-product of an interval and a polytope, which is then used in a two-step state estimation approach consisting of (i) state propagation (prediction) using the nonlinear system dynamics and (ii) measurement update (refinement) based on nonlinear observations. Moreover, we analyze the computational complexity of our proposed technique and derive sufficient conditions for stability of the estimation errors. Finally, we compare the effectiveness of our approach with existing polytopic and interval observers in the literature.**

***Index Terms*—Estimation, observers for nonlinear systems, uncertain systems, polytope-valued observers.**

I. Introduction

STATE estimation for systems where statistical characterization of uncertainties are not known/available has broad application in many research areas such as state-feedback control [1], localization [2] and fault detection and isolation [3]. The lack of (known) stochastic distributions in this setting renders particle and/or Kalman filtering-based approaches not applicable. Consequently, the literature considers the problem of state estimation in terms of computing guaranteed sets that contain true state trajectories and are compatible/consistent with system dynamics and constraints/observations.

Literature review: Several modifications to the commonly used *propagation-update* approach have been proposed for state estimation in dynamical systems in the presence of bounded but distribution-free uncertainties, where set-theoretic approaches are usually leveraged to compute enclosing sets of all possible system trajectories [4]. These methods consist of computing an enclosing set to the image set of the vector field of the system dynamics (propagation/prediction) and refining the obtained propagated set by finding an enclosure to its intersection with the set of states that are compatible/consistent with the observations/measurements (update).

However, it is well known that the computation of exact (tight) enclosures of sets that contain the evolution of the system states is in general intractable with complexity that grows exponentially with time, even for linear systems with polytopic initial and uncertainty sets [5]. Consequently, recent research focuses on developing set-theoretic approaches to tractably compute the tightest possible enclosures containing such sets. Several studies considered a trade-off by computing more conservative (i.e., outer-approximating) enclosures with lower computational complexity by assuming structurally simpler sets such as intervals [6], [7], hyperballs [8], [9], parallelotopes [10], or zonotopes [11]. In particular, zonotopic state estimation methods have been developed, e.g., in [12], based on first-order Taylor expansion, mean value extension or DC programming. However, the wrapping effect in interval-based approaches, as well as the symmetry of zonotopes in these techniques are sources of considerable conservatism, even when observation functions are linear.

To reduce the aforementioned conservatism, methods based on *constrained zonotopes* (CZ) [13] and *zonotope bundles* (ZB) [14], which are equivalent representations of polytopes, were introduced, where the key insight is to compute with sets in the space of generators of CZ and ZB that are intervals and hence, interval arithmetic could be directly applied [2]. Specifically, [4], [15] proposed CZ and ZB propagation and update algorithms for constrained discrete-time nonlinear systems based on mean value and first-order Taylor extensions of intervals, that are computationally efficient but potentially conservative due to the use of interval arithmetic. On the other hand, our recent work [16] proposed alternative CZ and ZB propagation and update approaches using mixed-monotone remainder-form decomposition functions [17]. By contrast, this letter considers the (direct) use of hyperplane and vertex representations of polytopes that can potentially return less conservative and faster results.

Contributions: This letter proposes novel methods for recursive state estimation using polytopes for bounded-error nonlinear discrete-time systems with nonlinear observation functions that (directly) use a combination of hyperplane (H) and vertex (V) representations of polytopes. First, we derive a tractable approach for finding the enclosure/outer-approximation of the

Manuscript received September 14, 2021; revised November 29, 2021; accepted December 19, 2021. Date of publication December 24, 2021; date of current version January 6, 2022. This work was supported in part by NSF under Grant CNS-1932066 and Grant CNS-1943545. Recommended by Senior Editor V. Ugrinovskii. *(Corresponding author: Sze Zheng Yong.)*

The authors are with the School for Engineering of Matter, Transport and Energy, Arizona State University, Tempe, AZ 85282 USA (e-mail: mkhajene@asu.edu; fshoaib@asu.edu; szyong@asu.edu).

Digital Object Identifier 10.1109/LCSYS.2021.3138355

set-product of an interval and a polytope, which naturally appears when applying the mean value theorem on nonlinear functions. Then, this result is leveraged to design a two-step state estimation approach consisting of state propagation (prediction) and measurement update (refinement) steps. In particular, the proposed propagation step that computes the predicted set of states in the next time step based on system dynamics is most efficiently computed using the V-representation of polytopes, while the update step that computes the intersection of the predicted set with the set of states that are compatible with uncertain observations via nonlinear observation functions can be more conveniently performed using its H-representation. Further, we derive sufficient stability conditions for the obtained polytope-valued estimates and analyze the computational complexity of our proposed technique. Finally, our proposed approaches are shown in several examples to yield the smallest set volumes when compared to existing approaches in the literature.

II. Preliminaries

Notation: $\mathbb{N}, \mathbb{N}_n, \mathbb{R}^n$ and $\mathbb{R}^{m\times n}$ denote the set of positive integers, $\{1,\dots,n\}$, the n-dimensional Euclidean space and the space of m by n real matrices, respectively. For $\mathcal{Z},\mathcal{W}\subset\mathbb{R}^n, R\in\mathbb{R}^{m\times n}, \mathcal{Y}\subset\mathbb{R}^m$, and $\mu{:}\mathbb{R}^n\to\mathbb{R}^m$, the following

$$R\mathcal{Z}\triangleq\{Rz|z\in\mathcal{Z}\},\ \mu(\mathcal{Z})\triangleq\{\mu(z)|z\in\mathcal{Z}\},\ \mathrm{Ver}(\mathcal{Z}),$$
$$\mathcal{Z}\oplus\mathcal{W}\triangleq\{z+w|z\in\mathcal{Z},w\in\mathcal{W}\},\ \mathcal{Z}\ominus\mathcal{W}\triangleq\mathcal{Z}\oplus(-\mathcal{W}),$$
$$\mathcal{Z}\cup_\mu\mathcal{Y}\triangleq\{z\in\mathcal{Z}|\mu(z)\in\mathcal{Y}\},\ \mathrm{int}(\mathcal{Z}),\ \mathrm{Proj}_n(\mathcal{Y})\ \text{and}$$
$$\mathrm{Conv}(\mathcal{Z})\triangleq\{\textstyle\sum_{i=1}^{n_z}\lambda_i z_i|z_i\in\mathcal{Z},\lambda_i\in[0,1],\sum_{i=1}^{n_z}\lambda_i=1,n_z\in\mathbb{N}\},$$

denote the linear mapping, general (nonlinear) mapping, the vertex set of (bounded) $\mathcal{Z}$, Minkowski sum, Pontryagin difference, generalized (nonlinear) intersection, interior of $\mathcal{Z}$, projection of $\mathcal{Y}$ onto the first n dimensions and convex hull of $\mathcal{Z}$, respectively. For $z\in\mathbb{R}^n$, $\|z\|_\infty\triangleq\max_{i\in\mathbb{N}_n}|z_i|$ denotes the ∞-norm of z, $z^+=\max\{z,0\}$ and $z^-=z^+-z$, while for $M,M'\in\mathbb{R}^{n\times m}$, $M\le M'$ denotes $M_{ij}\le M'_{ij}$ for all $i\in\mathbb{N}_n$ and $j\in\mathbb{N}_m$. Moreover, the transpose, Moore-Penrose pseudoinverse, (i,j)-th element, and spectral radius of R are given by $R^\top, R^\dagger, R_{(ij)}$ and $\rho(R)$, respectively. $\mathbb{B}^n_\infty\triangleq\{z\in\mathbb{R}^n|\|z\|_\infty\le 1\}$ is the ∞-norm unit hyperball and $\mathbb{D}_n$ is the set of n by n diagonal matrices.

Next, we formally define intervals, four different equivalent representations of polytopes and a new set operation that we will frequently use throughout this letter.

Definition 1 (Intervals): A set $\mathbb{I}\mathcal{Z}\subset\mathbb{R}^n$ is an interval in $\mathbb{R}^n$ if $\exists\underline{z},\overline{z}\in\mathbb{R}^n$ such that $\mathbb{I}\mathcal{Z}=[\underline{z},\overline{z}]\triangleq\{z\in\mathbb{R}^n|\underline{z}\le z\le\overline{z}\}$. An interval matrix can be defined similarly, in an element-wise manner. $\mathbb{IR}^n$ and $\mathbb{IR}^{n\times m}$ denote the sets of all intervals in $\mathbb{R}^n$ and $\mathbb{R}^{n\times m}$, respectively. Finally, $\mathrm{diam}(\mathbb{I}\mathcal{Z})\triangleq\overline{z}-\underline{z}$ denotes the diameter of the interval vector/matrix $\mathbb{I}\mathcal{Z}$.

Definition 2 (Polytopes): A set $\mathcal{P}\subset\mathbb{R}^n$ is a (convex) polytope, if it can be characterized via either of the following equivalent representations:

(i) *H-representation:* $\exists A_p\in\mathbb{R}^{n_p\times n}, b_p\in\mathbb{R}^{n_p}$ such that $\mathcal{P}=\{A_p,b_p\}_P\triangleq\{z\in\mathbb{R}^n|A_pz\le b_p\}$ is bounded;

(ii) *V-representation:* $\exists\mathcal{V}=\{v_1,\dots,v_p\}\triangleq\mathrm{Ver}(\mathcal{P})$, such that $\mathcal{P}=\mathrm{Conv}(\mathcal{V})$;

(iii) *Constrained Zonotope (CZ)-representation:* $\exists\tilde{G}\in\mathbb{R}^{n\times n_g},\tilde{c}\in\mathbb{R}^n,\tilde{A}\in\mathbb{R}^{n_c\times n_g},\tilde{b}\in\mathbb{R}^{n_c}$ such that $\mathcal{P}=\{\tilde{G},\tilde{c},\tilde{A},\tilde{b}\}_{CZ}\triangleq\{\tilde{G}\xi+\tilde{c}|\xi\in\mathbb{B}^{n_g},\tilde{A}\xi=\tilde{b}\}$ with n_g generators and n_c constraints;

(iv) *Zonotope Bundle (ZB)-representation:* $\exists\{G_s\in\mathbb{R}^{n\times\hat{n}_s},c_s\in\mathbb{R}^n\}_{s=1}^S$ such that $\mathcal{P}=\cap_{s=1}^S\{G_s,c_s\}_Z\triangleq\cap_{s=1}^S\{G_s\zeta+c_s|\zeta\in\mathbb{B}^{\hat{n}_s}\}$, with $\hat{n}_s$ generators for each zonotope $\{G_s,c_s\}_Z, s=1,\dots,S$.

It is worth mentioning that the CORA 2020 toolbox [18] can exactly convert polytopes among all the above representations, including the transformation between H- and V-representations that is frequently used in this letter, summarized as:

$$\mathcal{P}=\{A_p,b_p\}_P\overset{\text{H-V}}{\Longleftrightarrow}\mathrm{Conv}(\mathrm{Ver}(\mathcal{P})).$$

Definition 3 (Set-Product): For an interval matrix $\mathbb{J}\in\mathbb{IR}^{m\times n}$ and a set $\mathcal{P}\subset\mathbb{R}^n$, $\mathcal{S}=\mathbb{J}\odot\mathcal{P}\triangleq\{s\in\mathbb{R}^m|s=Jp,J\in\mathbb{J},p\in\mathcal{P}\}$ is called the set-product of $\mathbb{J}$ and $\mathcal{P}$.

Finally, we present two propositions, which will be used later to derive the main results of the letter.

Proposition 1: Suppose $\mathcal{Z}_1,\dots,\mathcal{Z}_{n_z}$ are $n_z\in\mathbb{N}$ (convex) polytopes with vertex sets $\mathcal{V}_1=\mathrm{Ver}(\mathcal{Z}_1),\dots,\mathcal{V}_{n_z}=\mathrm{Ver}(\mathcal{Z}_{n_z})$. Let us define $\mathcal{S}\triangleq\mathrm{Conv}(\mathcal{Z}_1,\dots,\mathcal{Z}_{n_z})\triangleq\{\sum_{i=1}^{n_z}\lambda_i z_i|z_i\in\mathcal{Z}_i,\lambda_i\in[0,1],\sum_{i=1}^{n_z}\lambda_i=1\}$. Then, the following inclusion holds: $\mathcal{S}\subseteq\mathrm{Conv}(\bigcup_{i=1}^{n_z}\mathcal{V}_i)$.

Proof: Let $s\in\mathcal{S}$. Then, by the definition of $\mathcal{S}$,

$$s=\sum_{i=1}^{n_z}\lambda_i z_i,\ \text{for some}\ \lambda_i\in[0,1],z_i\in\mathcal{Z}_i,\ \text{s.t.}\ \sum_{i=1}^{n_z}\lambda_i=1.\quad(1)$$

On the other hand, by convexity of $\mathcal{Z}_i$'s, each z_i can be represented as a convex combination of the members of $\mathcal{V}_i$. In other words, $z_i=\sum_{j=1}^{|\mathcal{V}_i|}\alpha_j^i v_j^i$, where $v_j^i\in\mathcal{V}_i,\alpha_j^i\in[0,1],\sum_j^{|\mathcal{V}_i|}\alpha_j^i=1$ and $|\mathcal{V}_i|$ is the cardinality of $\mathcal{V}_i$. Combining this and (1), we find that $s=\sum_{i=1}^{n_z}\sum_{j=1}^{|\mathcal{V}_i|}\lambda_i\alpha_j^i v_j^i$, where $v_j^i\in\mathcal{V}_i,\lambda_i,\alpha_j^i\in[0,1],\sum_j^{|\mathcal{V}_i|}\alpha_j^i=1,\sum_{i=1}^{n_z}\lambda_i=1$, which implies that s is a *linear* combination of $v_j^i\in\bigcup_i^{n_z}\mathcal{V}_i$. To show that it is also a *convex* combination, first note that $\lambda_i\alpha_j^i\in[0,1]$, since $\lambda_i\in[0,1]$ and $\alpha_j^i\in[0,1]$. Moreover, $\sum_{i=1}^{n_z}\sum_{j=1}^{|\mathcal{V}_i|}\lambda_i\alpha_j^i=\sum_{i=1}^{n_z}\lambda_i\sum_{j=1}^{|\mathcal{V}_i|}\alpha_j^i=\sum_{i=1}^{n_z}\lambda_i=1$. Hence, s can be represented as a convex combination of the union of the vertex sets $\mathcal{V}_i$'s, i.e., $s\in\mathrm{Conv}(\bigcup_{i=1}^{n_z}\mathcal{V}_i)$. This, completes the proof. ■

Proposition 2: Let $A\in[\underline{A},\overline{A}]\subset\mathbb{IR}^{m\times n}$ and $x\in\mathbb{R}^n$. Then, $\underline{A}x^+-\overline{A}x^-\le Ax\le\overline{A}x^+-\underline{A}x^-$. As a corollary, if $x\ge 0$, then $\underline{A}x\le Ax\le\overline{A}x$, and if $x\le 0$, then $\overline{A}x\le Ax\le\underline{A}x$.

Proof: The proof is similar to the proof of [7, Lemma 1], with changed roles of A and x, since here, A is the uncertain variable (matrix) and x is a fixed vector. ■

III. Problem Formulation

System Assumptions: Consider the following bounded-error nonlinear constrained discrete-time system:

$$x_{k+1}=\hat{f}(x_k,w_k,u_k)=f(z_k),$$
$$\hat{\mu}(x_k,u_k)=\mu(x_k)\in\mathcal{Y}_k,\ x_0\in\mathcal{X}_0,w_k\in\mathcal{W}_k,\quad(2)$$

where $z_k\triangleq[x_k^\top w_k^\top]^\top$, $x_k\in\mathbb{R}^{n_x}$ is the state vector, $w_k\in\mathcal{W}_k\subset\mathbb{R}^{n_w}$ is the augmentation of all exogenous uncertain inputs, e.g., bounded process disturbance/noise and internal uncertainties such as uncertain parameters and $u_k\in\mathcal{U}_k\subseteq\mathbb{R}^{n_u}$ is the *known* input signal. Moreover, $f:\mathbb{R}^{n_z}\to\mathbb{R}^{n_x}$ (with $n_z\triangleq n_x+n_w$) and $\mu:\mathbb{R}^{n_x}\to\mathbb{R}^{n_\mu}$ are the nonlinear state vector field and the observation/constraint mapping, respectively, which are well-defined since u_k in $\hat{f}(\cdot,\cdot)$ and $\hat{\mu}(\cdot,\cdot)$ are assumed to be known. Note that the mapping

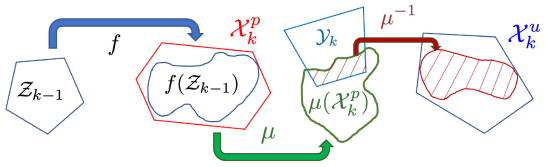

Fig. 1. Illustration of propagation and update steps in (3) and (4).

$\mu(\cdot)$ along with the set $\mathcal{Y}_k$ characterize all a priori known or manufactured/redundant constraints over the states, uncertain observations (with bounded measurement noise) or uncertain parameters at time k. Moreover, we assume the following.

Assumption 1: $\mathcal{X}_0$ and $\mathcal{W}_k$, $\mathcal{Y}_k$, $\forall k \geq 0$ are polytopes.

Assumption 2: The nonlinear vector fields $f(\cdot)$ and $\mu(\cdot)$ are locally Lipschitz on their domains. Consequently, they are differentiable and have bounded Jacobian matrix elements, almost everywhere. We further assume that given any $\mathcal{Z} \subset \mathbb{R}^{n_z}$ and $\mathcal{X} \subset \mathbb{R}^{n_x}$, some upper and lower bounds for all elements of the Jacobian matrices of $f(\cdot)$ and $\mu(\cdot)$ over $\mathcal{Z}$ and $\mathcal{X}$ are available or can be computed. In other words, $\exists \underline{J}_f, \overline{J}_f \in \mathbb{R}^{n_x \times n_z}, \underline{J}_\mu, \overline{J}_\mu \in \mathbb{R}^{n_\mu \times n_x}$, such that: $\underline{J}_f \leq J_f(z) \leq \overline{J}_f, \underline{J}_\mu \leq J_\mu(x) \leq \overline{J}_\mu, \forall z \in \mathcal{Z}, \forall x \in \mathcal{X}$, where $J_f(z)$ and $J_\mu(x)$ denote the Jacobian matrices of the mappings $f(\cdot)$ and $\mu(\cdot)$ at the points z and x, respectively.

Our goal is to design novel set-membership approaches for obtaining set-valued state estimates for bounded-error nonlinear systems in the form of (2). In particular, we consider a two-step approach consisting of i) propagation (prediction) and ii) update (refinement) steps, where at each time step $k \in \mathbb{N}$, we seek to solve the following problems:

Problem 1 (Propagation): Given the 'updated set' $\mathcal{X}_{k-1}^u$ from the previous time step and $\mathcal{W}_{k-1}$ (with $\mathcal{Z}_{k-1} \triangleq \mathcal{X}_{k-1}^u \times \mathcal{W}_{k-1}$), find the 'propagated set' $\mathcal{X}_k^p$ that satisfies

$$f(\mathcal{Z}_{k-1}) \triangleq \{\hat{f}(x, w, u_{k-1}) | x \in \mathcal{X}_{k-1}^u, w \in \mathcal{W}_k\} \subseteq \mathcal{X}_k^p. \quad (3)$$

Problem 2 (Update): Given the 'propagated set' $\mathcal{X}_k^p$ and the uncertain observation/constraint set $\mathcal{Y}_k$ at time step k, find the 'updated set' $\mathcal{X}_k^u$ that satisfies

$$\mathcal{X}_k^p \cap_\mu \mathcal{Y}_k \triangleq \{x \in \mathcal{X}_k^p | \mu(x) \in \mathcal{Y}_k\} \subseteq \mathcal{X}_k^u. \quad (4)$$

Figure 1 schematically illustrates the propagation and update steps in (3) and (4). In a previous work [16], we addressed these problems using (indirect) CZ- and ZB-representations of the polytopes (cf. Definition 2-(iii), (iv)). In this letter, we consider them using a combination of (direct) H- and V-representations (cf. Definition 2-(i), (ii)).

IV. Direct Polytopic Set Computation

As above-mentioned, we consider a *recursive* two-step state estimation approach consisting of state propagation (prediction) and measurement update (refinement) steps by solving Problems 1 and 2. Our recursive algorithm can be either initialized at time 0 with the initial polytopic state estimate $\mathcal{X}_0$ as $\mathcal{X}_0^u = \mathcal{X}_0$ or if $\mathcal{Y}_0$ is available/measured, with $\mathcal{X}_0^p = \hat{\mathcal{X}}_0$ and the application of the update step by solving Problem 2 at time 0 to obtain $\mathcal{X}_0^u$. At each time step k, beginning with the updated set $\mathcal{X}_{k-1}^u$ from the previous time step in the V-representation, we find the propagated set $\mathcal{X}_k^p$ by solving Problem 1. As will be described in Section IV-B, this propagation step is most efficiently computed using the V-representation of polytopes, hence, $\mathcal{X}_{k-1}^u$ is first converted into its equivalent V-representation, e.g., by using CORA [18], if necessary, for this step. Next, given the uncertain observation/constraint set $\mathcal{Y}_k$, we find the updated set $\mathcal{X}_k^u$ by solving Problem 2. This update step will be shown in Section IV-C to be more conveniently performed using the H-representation of polytopes and it involves the exact conversion from V-representation of a certain set into its H-representation, e.g., by using CORA [18]. Since this recursive approach involves the use of and conversion between (direct) V- and H- representations of polytopes, for simplicity, we will refer to this approach as the direct polytopic V-H approach.

A. Set-Product Bounding

A key component of our approach to solve Problems 1 and 2 is via the application of the mean value theorem (in set-theoretic form) on the nonlinear functions $f(\cdot)$ and $\mu(\cdot)$ in (2), where a set-product of an interval and a polytope naturally appears since the Jacobian matrices are given as intervals (cf. Assumption 2). Hence, we first state a result on bounding/enclosing/outer-approximating the set-product (cf. Definition 3) of an interval matrix and a polytope in the H-representation, through the following lemma.

Lemma 1 (Set-Product Bounding): Let $\mathcal{P} \subset \mathbb{R}^n$ be a polytope with the vertex set $\text{Ver}(\mathcal{P}) = \{v_i\}_{i=1}^{n_P}$ and $\mathbb{J} = [\underline{J}, \overline{J}] \in \mathbb{IR}^{m \times n}$ be an interval matrix, with $\text{Ver}(\mathbb{J}) \triangleq \{J \in \mathbb{R}^{m \times n} | J_{ij} = \underline{J}_{ij} \vee J_{ij} = \overline{J}_{ij}, 1 \leq i \leq n, 1 \leq j \leq m\}$. Then, the following inclusion holds:

$$\mathbb{J} \odot \mathcal{P} \subseteq \text{Conv}\Big(\bigcup_{i=1}^{n_P} \text{Ver}(\mathbb{S}_i)\Big), \quad (5)$$

where $\mathbb{S}_i \triangleq [\underline{J}v_i^+ - \overline{J}v_i^-, \overline{J}v_i^+ - \underline{J}v_i^-], \ \forall i \in \mathbb{N}_{n_P}$.

Proof: Let $s \in \mathbb{J} \odot \mathcal{P}$. By Definition 3, $\exists p \in \mathcal{P}$ and $J \in [\underline{J}, \overline{J}]$ such that

$$s = Jp = \sum_{i=1}^{n_p} \lambda_i J v_i, \ \text{ for some } \lambda_i \in [0, 1], \sum_{i=1}^{n_p} \lambda_i = 1. \quad (6)$$

On the other hand, from Proposition 2, $Jv_i \in \mathbb{S}_i$. Combining this with (6) results in $s \in \text{Conv}(\mathbb{S}_1, \ldots, \mathbb{S}_{n_P})$, from which we obtain $s \in \text{Conv}(\bigcup_{i=1}^{\mathbb{N}_P} \text{Ver}(\mathbb{S}_i))$ using Proposition 1. ■

B. Polytopic Propagation

Now, equipped with Lemma 1, we propose a solution to Problem 1 that combines Lemma 1 and Proposition 2 to find a polytopic inclusion for the range/image set of the vector field $f(\cdot)$ in (2), when its domain is the polytope $\mathcal{P}$ in the form of a convex combination of vertex sets of hyper-intervals. The following theorem formally summarizes this result, where the solution to Problem 1 can be found as $\mathcal{X}_k^p = \mathcal{P}_f$ given $\mathcal{P} = \mathcal{X}_{k-1}^u \times \mathcal{W}_{k-1}$.

Theorem 1 (Direct Polytopic Propagation): Suppose $f : \mathbb{R}^{n_z} \to \mathbb{R}^{n_x}$ satisfies Assumption 2 (i.e., $J_f(x) \in \mathbb{J}_f \triangleq [\underline{J}_f, \overline{J}_f], \forall x \in \mathcal{X}$ with known $\mathbb{J}_f$), and let $\mathcal{P}$ be a polytope in $\mathbb{R}^{n_z}$ with the vertex set $\text{Ver}(\mathcal{P}) = \{v_i\}_{i=1}^{n_P}$. Then, for an arbitrary point in the interior of the polytope $\mathcal{P}$, i.e., $p_0 \in \text{int}(\mathcal{P})$, the following set inclusion holds:

$$f(\mathcal{P}) \subseteq \text{Conv}\Big(\bigcup_{i=1}^{n_P} \text{Ver}(\tilde{\mathbb{S}}_i)\Big) \triangleq \mathcal{P}_f, \quad (7)$$

where $\tilde{\mathbb{S}}_i \triangleq [\underline{J}_f\tilde{v}_i^+ - \overline{J}_f\tilde{v}_i^- + f(p_0), \overline{J}_f\tilde{v}_i^+ - \underline{J}_f\tilde{v}_i^- + f(p_0)]$ and $\tilde{v}_i \triangleq v_i \ominus p_0$, $\forall i \in \mathbb{N}_{n_P}$.

Proof: By applying a generalized version of the mean value theorem [19] to the nonlinear function $f(\cdot)$ and using Lemma 1 to bound the resulting set-product, we obtain: $f(\mathcal{P}) \subseteq f(p_0) \oplus \mathbb{J}_f \odot (\mathcal{P}_f \ominus p_0) \subseteq \text{Conv}(\bigcup_{i=1}^{n_P} \text{Ver}(\tilde{\mathbb{S}}_i))$. ■

Note that the above approach for state propagation uses the vertices of $\mathcal{P} = \mathcal{X}_{k-1}^u \times \mathcal{W}_{k-1}$ (i.e., in V-representation), and the resulting set $\mathcal{X}_k^p = \mathcal{P}_f$ is also in its V-representation.

C. Polytopic Update

Next, we address Problem 2 by proposing a method for computing the updated set estimate $\mathcal{X}_k^u$ by intersecting the predicted set $\mathcal{X}_k^p$ with the set of states that are compatible with uncertain observations/constraints $\mathcal{Y}_k$ and the polytopic inclusion for the range/image set of the nonlinear observation function $\mu(\cdot)$ in (2). This can be achieved, as shown in the following theorem, with $\mathcal{P}_f = \mathcal{X}_k^p$ in both V- and H-representations (with conversion using CORA [18], if necessary) and $\mathcal{P}_\mu = \mathcal{Y}_k$ in its H-representation as inputs and $\mathcal{X}_k^u = \mathcal{P}_u$ is the resulting updated set.

Theorem 2 (Polytopic Update): Suppose $\mu : \mathbb{R}^{n_x} \to \mathbb{R}^{n_\mu}$ satisfies Assumption 2 and let $\mathcal{P}_f \triangleq \{A_f, b_f\}_P \overset{\text{H-V}}{\iff} \text{Conv}(\{v_i\}_{i=1}^{n_f}) \subset \mathbb{R}^{n_x}$ and $\mathcal{P}_\mu \triangleq \{A_\mu, b_\mu\}_P \subset \mathbb{R}^{n_\mu}$ be two polytopes in V- and H-representations (cf. Definition 1), with $A_f \in \mathbb{R}^{m_x \times n_x}$, $A_\mu \in \mathbb{R}^{m_\mu \times n_\mu}$. For all $x \in \mathbb{R}^{n_x}$, define $\phi(x) \triangleq A_\mu \mu(x)$ and suppose that $J_\phi(x) \in \mathbb{J}_\phi \triangleq [\underline{J}_\phi, \overline{J}_\phi], \forall x \in \mathcal{X}$, where $J_\phi(x)$ is the Jacobian matrix of $\phi(x)$ at $x \in \mathcal{X}$ and the interval matrix $\mathbb{J}_\phi$ is known (or computed with interval arithmetic). Then, for any $q_0 \in \text{int}(\mathcal{P}_f)$, the following set inclusion holds:

$$\mathcal{P}_f \cap_\mu \mathcal{P}_\mu \subseteq \mathcal{P}_u \triangleq \text{Proj}_{n_x}(\{A_u, b_u\}_P), \tag{8}$$

where $A_u \triangleq \begin{bmatrix} -J_\phi^m & I \\ A_f & 0 \\ 0 & \tilde{A} \end{bmatrix}$, $b_u \triangleq \begin{bmatrix} b_\mu + J_\phi^m q_0 - \phi(q_0) \\ b_f \\ \tilde{b} \end{bmatrix}$.

Further,

$$\text{Conv}\Big(\bigcup_{i=1}^{n_f} \text{Ver}(\tilde{\mathbb{W}}_i)\Big) \overset{\text{V-H}}{\iff} \{\tilde{A}, \tilde{b}\}_P, \tag{9}$$

with $\tilde{\mathbb{W}}_i \triangleq \frac{1}{2}[-\text{diam}(\mathbb{J}_\phi)|\tilde{v}_i|, \text{diam}(\mathbb{J}_\phi)|\tilde{v}_i|]$, $\tilde{v}_i \triangleq v_i - q_0$, $J_\phi^m \triangleq \frac{1}{2}(\underline{J}_\phi + \overline{J}_\phi)$ and $\text{diam}(\mathbb{J}_\phi) = \overline{J}_\phi - \underline{J}_\phi$.

Proof: First, note that by definition, $\mathcal{P}_f \cap_\mu \mathcal{P}_\mu = \{x \in \mathcal{P}_f | \mu(x) \in \mathcal{P}_\mu\} = \{x \in \mathcal{P}_f | A_\mu \mu(x) \leq b_\mu\} = \{x \in \mathcal{P}_f | \phi(x) \leq b_\mu\}$. So, our goal is to show that $\{x \in \mathcal{P}_f | \phi(x) \leq b_\mu\} \subseteq \mathcal{P}_u$. To do this, we first apply the mean value theorem to obtain the following: $\phi(\mathcal{P}_f) \subseteq \phi(q_0) \oplus \mathbb{J}_\phi \odot (\mathcal{P}_f \ominus q_0)$. On the other hand, the interval matrix $\mathbb{J}_\phi$ can be decomposed as $\mathbb{J}_\phi = J_\phi^m \oplus \mathbb{J}_\phi^\Delta$ with $\mathbb{J}_\phi^\Delta = \frac{1}{2}[-\text{diam}(\mathbb{J}_\phi), \text{diam}(\mathbb{J}_\phi)]$ and J_ϕ^m and $\text{diam}(\mathbb{J}_\phi)$ given in (9). Plugging this back into the above enclosure results in

$$\phi(\mathcal{P}_f) \subseteq (\phi(q_0) - J_\phi^m q_0) \oplus J_\phi^m \mathcal{P}_f \oplus \mathbb{J}_\phi^\Delta \odot (\mathcal{P}_f \ominus q_0). \tag{10}$$

Then, we apply Lemma 1 to the set-product $\mathbb{J}_\phi^\Delta \odot (\mathcal{P}_f \ominus q_0)$ to obtain the enclosure $\text{Conv}(\bigcup_{i=1}^{n_f} \text{Ver}(\tilde{\mathbb{W}}_i))$, as well as its conversion to its H-representation, $\{\tilde{A}, \tilde{b}\}_P$, i.e.,

$$\mathbb{J}_\phi^\Delta \odot (\mathcal{P}_f \ominus q_0) \subseteq \text{Conv}\Big(\bigcup_{i=1}^{N_f} \text{Ver}(\tilde{\mathbb{W}}_i)\Big) \overset{\text{V-H}}{\iff} \{\tilde{A}, \tilde{b}\}_P, \tag{11}$$

TABLE I
COMPLEXITY OF THE PROPOSED PREDICTION AND UPDATE STEPS

Steps	Complexity
Prediction	$O(n_P(n_x(n_x+n_w)^2 + 2^{n_x}))$
Update	$O(m_x n_f^3 (n_x^2 m_x + 2^{m_x})^3 + n_h^{2^{n_h}})$

with $\mathbb{W}_i$ given in (9). Combining (10) and (11) yields:

$$\{x \in \mathcal{P}_f | \phi(x) \leq b_\mu\} \subseteq \mathcal{P}_u, \tag{12}$$

where $\mathcal{P}_u \triangleq \{x \in \mathbb{R}^{n_x} \mid A_f x \leq b_f, \exists z \in \mathbb{R}^{m_\mu}, s.t.\ \tilde{A}z \leq \tilde{b} \wedge \phi(q_0) - J_\phi^m q_0 + J_\phi^m x + z \leq b_\mu\}$. In the above, augmenting the affine constraints in $\mathcal{P}_u$ results in a lifted polytope $\{A_u, b_u\}_P$, whose projection onto the first n_x dimensions, i.e., the state space, is equivalent to $\mathcal{P}_u$, by construction. ■

V. Uniform Boundedness of Estimates

In this section, we investigate the stability/convergence of the obtained polytopic enclosures through Theorem 3, for which we only provide a proof sketch due to space limitation. To do so, we first define the notion of stability we consider.

Definition 4 (Stability): A sequence of polytopes $\{\mathcal{P}_k\}_{k=0}^\infty$ is called stable, if there exists a sequence of enclosing intervals $\{\mathbb{IX}_k \triangleq [\underline{x}_k, \overline{x}_k]\}_{k=0}^\infty$, such that each $\mathbb{IX}_k$ is an enclosing interval to the polytope $\mathcal{P}_k$ (i.e., $\mathcal{P}_k \subseteq \mathbb{IX}_k$) and $\{\|\Delta x_k\|_\infty \triangleq \|\overline{x}_k - \underline{x}_k\|_\infty\}_{k=0}^\infty$ is a uniformly bounded sequence.

Theorem 3 (Stability): Suppose all assumptions in Theorems 1 and 2 hold and without loss of generality, $\underline{J}_f = -\overline{J}_f$. Then, the sequence of $\{\mathcal{X}_k^u\}_{k=0}^\infty$ is stable if $\min_{D \in \mathbb{D}_{n_x}^r} \rho(\mathcal{L}(D)) < 1$, where $\mathbb{D}_{n_x}^r \triangleq \{D \in \mathbb{D}_{n_x} \mid \forall i \in \mathbb{N}_{n_x}, D_{(ii)} = 0$ if the i-th row of $I - J_\phi^{m\dagger} J_\phi^m$ is not zero$\}$, and $\mathcal{L}(D) \triangleq D|J_\phi^{m\dagger}|(\frac{1}{2}\text{diam}(\mathbb{J}_\phi) + 2|J_\phi^m|\overline{J}_f) + 2(I - D)\overline{J}_f$.

Proof: (Sketch) Starting from an initial polytope $\mathcal{P}_0 = \text{Conv}(\{\tilde{v}_i\}_{i=1}^n)$, by sequentially applying the polytopic propagation and update steps in Theorems 1 and 2, we obtain a stable sequence of polytopes, through the following steps:

1) $\mathcal{P}_0 \subseteq \mathbb{IX}_0 \triangleq [\min_{i \in \mathbb{N}_n}\{\tilde{v}_i\}, \max_{i \in \mathbb{N}_n}\{\tilde{v}_i\}]$ with $\Delta x_0 \geq \max_{i \in \mathbb{N}_n} |\tilde{v}_i|$;
2) $\mathcal{P}_u \subseteq \mathbb{IX}_f \triangleq \overline{J}_f \odot [-\max_{i \in \mathbb{N}_n} |\tilde{v}_i|, \max_{i \in \mathbb{N}_n} |\tilde{v}_i|]$;
3) $\mathcal{P}_u \subseteq \mathbb{IX}_u \triangleq [(J_\phi^{m\dagger})^+\underline{\zeta} - (J_\phi^{m\dagger})^-\overline{\zeta} - \kappa r, (J_\phi^{m\dagger})^+\overline{\zeta} - (J_\phi^{m\dagger})^-\underline{\zeta} + \kappa r]$, where $\underline{\zeta} \triangleq J_\phi^{m+}\underline{x}_f - J_\phi^{m-}\overline{x}_f$, $\overline{\zeta} \triangleq c + \frac{1}{2}\text{diam}(\mathbb{J}_\phi)\max_{i \in \mathbb{N}_n} |\tilde{v}_i|$, $\kappa = \infty$, $c \triangleq b_\mu - \phi(q_0) + J_\phi^m q_0$;
4) $\mathcal{P}_u$ is included in an interval whose diameter is less than $\min(\Delta x_f, \Delta x_u) \leq D\Delta x_u + (I - D)\Delta x_f, \forall D \in \mathbb{D}_{n_x}$;
5) If $D \in \mathbb{D}_{n_x}^r$, then $\Delta x_k \leq \mathcal{L}(D)\Delta x_{k-1} + D|J^{m\dagger}|c$. ■

VI. Complexity Analysis

In this section, we study the worst-case complexity analysis of our proposed polytopic state estimator, namely for each of the propagation and update steps, and the results are summarized in Table I. For the complexity analysis of the propagation step, we assume that $\mathcal{Z}_{k-1} = \mathcal{X}_{k-1}^u \times \mathcal{W}_{k-1} \subset \mathbb{R}^{n+n_w}$ is already given in its V-representation with n_P vertices. Then, the complexity of the propagation step in Theorem 1 consists of $O(n_x(n_x + n_w)^2)$ for finding each interval matrix $\mathbb{S}_i$ and $O(2^{n_x})$ for enumerating the vertices of each $\mathbb{S}_i$, resulting in a total of $O(n_P(n_x(n_x + n_w)^2 + 2^{n_x}))$.

On the other hand, for the complexity analysis of the update step, we assume that $\mathcal{X}_k^p \subset \mathbb{R}^{n_x}$ is given in both H- and

V-representations with m_x constraints and n_f vertices, respectively, and $\mathcal{Y}_k \subset \mathbb{R}^{n_\mu}$ is in H-representation with m_μ constraints/facets. In this case, the complexity for computing each interval matrix and its vertex enumerations, $\tilde{\mathbb{W}}_i$, is $O(n_x^2 m_x)$ and $O(2^{m_x})$, respectively, which brings the complexity for finding $\bigcup_{i=1}^{n_f} \text{Ver}(\tilde{\mathbb{W}}_i)$ in Theorem 2 to $O(n_f(n_x^2 m_x + 2^{m_x}))$. Then, its conversion to H-representation has a complexity of $O(m_x n_f^3 (n_x^2 m_x + 2^{m_x})^3)$ with at most $n_h \leq n_f^2 (n_x^2 m_x + 2^{m_x})^2$ facets/constraints (i.e., $\tilde{A} \in \mathbb{R}^{n_h \times n_x}$) [20]. Finally, the projection operation has a complexity of $O(n_h^{2^{n_h}})$ when using the Fourier-Motzkin method, leading to the total complexity in Table I, which is relatively high in the worst-case but is often faster in practice, as shown in the simulation examples in the following section.

VII. Simulations

In this section, we compare the performance of the proposed state estimation approach with several existing methods in the literature in terms of computational time and volume of obtained enclosures. All computations are conducted on a single Intel core i5-8250U 1.6 GHz CPU with 8 GB memory, using MATLAB 2020b. We compare the following polytope-valued estimation methods: i) RRSR, i.e., the mean value extension-based technique introduced in [4], ii) V-H, i.e., the direct polytopic set computation introduced in Section IV, iii) D-ZB, i.e., decomposition-based propagation and update with ZBs proposed in our previous work [16] and iv) D-CZ, i.e., decomposition-based propagation and update with CZs that was also introduced in [16], using a two dimensional nonlinear benchmark system from [4], followed by a three dimensional unicycle system from [21]. Note that $\overline{J}_\mu, \underline{J}_\mu$ is computed via interval arithmetic using CORA 2020 toolbox [18]. The corresponding computation time as well as the time required for conversion between V- and H-representations are included in the results below.

A. Example I (Benchmark System in [4])

Consider the following discrete-time system [4]:

$$\begin{aligned} x_{1,k} &= 3x_{1,k-1} - \frac{x_{1,k-1}^2}{7} - \frac{4x_{1,k-1}x_{2,k-1}}{4 + x_{1,k-1}} + w_{1,k-1}, \\ x_{2,k} &= -2x_{2,k-1} + \frac{3x_{1,k-1}x_{2,k-1}}{4 + x_{1,k-1}} + w_{2,k-1}, \\ y_{1,k} &= x_{1,k} + v_{1,k}, \;\; y_{2,k} = -x_{1,k} + x_{2,k} + v_{2,k}, \end{aligned} \tag{13}$$

with $\|w_k\|_\infty \leq 0.1$, $\|v_k\|_\infty \leq 0.4$, and an initial zonotope that includes the the initial state, $\mathcal{X}_0 = \left\{ \begin{bmatrix} 0.1 & 0.2 & -0.1 \\ 0.1 & 0.1 & 0 \end{bmatrix}, \begin{bmatrix} 0.5 \\ 0.5 \end{bmatrix} \right\}_Z$.

Figure 2 depicts the obtained polytope-valued estimates for time steps $k = 0, \ldots, 4$ using the four aforementioned approaches. As can be observed, the enclosures obtained using the proposed V-H method are the least conservative for all time steps, presumably since approximation errors incurred by the use of decomposition functions in the D-CZ and D-ZB approaches can be avoided. Moreover, the results attained by the D-CZ approach are quite similar to the ones by RRSR. The resulting sets from intersecting the sets from all approaches at each time step (COMB method) were also plotted in Figure 2 to illustrate the best possible estimates. For further comparison, the average computation times and average volumes of

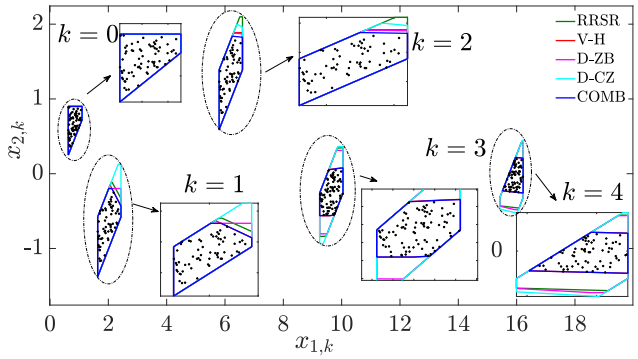

Fig. 2. Results for the first four time steps of the different polytope-valued state estimation methods in Example I. Black dots are obtained from uniform sampling of $\mathcal{X}_0$ and their propagation through the vector field. Note that the red sets from the V-H method lie almost exactly behind the blue sets obtained from intersecting the sets from all methods at each time step.

TABLE II
Average Computation Times (in Seconds) and Average Volumes of the Set Estimates at Each Time Step for Example I Using Various Estimation Approaches. Averages Are Taken Over 50 Simulation Runs With Random Noise

Methods:		$k=0$	$k=1$	$k=2$	$k=3$	$k=4$
RRSR	Time:	0.0866	1.0000	0.9241	0.9321	0.9890
	Vol.:	0.3496	0.5926	0.6288	0.5780	0.4120
V-H	Time:	0.0672	0.7030	0.6655	0.6140	0.7031
	Vol.:	0.3496	0.5489	0.5826	0.4077	0.2306
D-ZB	Time:	0.0709	3.5132	3.5092	2.8569	4.0240
	Vol.:	0.3496	0.5691	0.5877	0.5661	0.4266
D-CZ	Time:	0.0711	2.0940	3.5201	2.8575	2.5850
	Vol.:	0.3496	0.6226	0.6077	0.5936	0.4676
COMB	Time:	0.0710	7.0943	6.9250	6.9278	7.5850
	Vol.:	0.3496	0.5405	0.5625	0.4033	0.2302

the set estimates from 50 runs using the different methods are given in Table II, where the V-H approach is the fastest and also yields the most accurate estimates, i.e., with the smallest volumes at each time step. Moreover, we also tried to implement the interval observer in [6] on this example. However, the interval observer design did not result in any feasible observer gain, and when we modified the system such that [6] is applicable, we observed that the sets obtained by [6] had volumes that were often 100 times larger than those obtained by the V-H approach.

B. Example II (Unicycle System in [21])

Next, we consider the discretized unicycle-like mobile robot system [21], as follows:

$$\begin{aligned} s_{x,k+1} &= s_{x,k} + T_0 \phi_w \cos(\theta_k) + w_{1,k}, \\ s_{y,k+1} &= s_{y,k} + T_0 \phi_w \sin(\theta_k) + w_{2,k}, \\ \theta_{k+1} &= \theta_k + T_0 \phi_\theta + w_{3,k}, \\ y_k &= [d_{1,k} \;\; \phi_{1,k} \;\; d_{2,k} \;\; \phi_{2,k}]^\top + v_k, \end{aligned} \tag{14}$$

where $x_k \triangleq [s_{x,k}\, s_{y,k}\, \theta_k]^\top$, $w_k = [w_{x,k}\, w_{y,k} \;\; w_{\theta,k}]^\top$, $\phi_{\omega,k} = 0.3$, $\phi_{\theta,k} = 0.15$, $w_{x,k} = 0.2(0.5\rho_{x_{1,k}} - 0.3)$, $w_{y,k} = 0.2(0.3\rho_{x_{2,k}} - 0.2)$ and $w_{\theta,k} = 0.2(0.6\rho_{x_{3,k}} - 0.4)$, with $\rho_{x_{l,k}} \in [0, 1]$ $(l = 1, 2, 3)$ and initial state $x_0 = [0.1 \;\; 0.2 \;\; 1]^\top$. Moreover, $\forall i \in \{1, 2\}$, $d_{i,k} = \sqrt{(s_{x_i} - s_{x,k})^2 + (s_{y_i} - s_{y,k})^2}$ and $\phi_{i,k} = \theta_k - \arctan(\frac{s_{y_i} - s_{y,k}}{s_{x_i} - s_{x,k}})$, with s_{x_i}, s_{y_i} being two

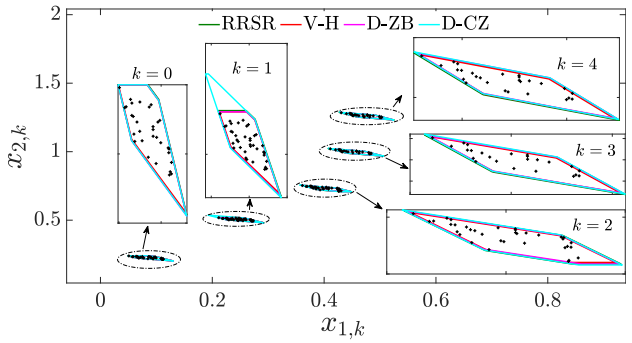

Fig. 3. Results for the first four time steps of the different polytope-valued state estimation methods in Example II. Black dots are obtained from uniform sampling of $\mathcal{X}_0$ and their propagation through the vector field.

TABLE III
AVERAGE COMPUTATION TIMES (IN SECONDS) AND AVERAGE VOLUMES OF THE SET ESTIMATES (WITH A FACTOR OF 10^{-4}) AT EACH TIME STEP FOR EXAMPLE II USING VARIOUS ESTIMATION APPROACHES. AVERAGES ARE TAKEN OVER 20 SIMULATION RUNS WITH RANDOM NOISE

Methods:		$k=0$	$k=1$	$k=2$	$k=3$	$k=4$
RRSR	Time:	0.5640	0.8780	0.9654	0.8964	1.8071
	Vol.:	0.3022	0.4012	0.3022	0.4002	0.3021
V-H	Time:	1.1080	59.9411	59.2030	60.4890	69.1305
	Vol.:	0.3000	0.3001	0.4000	0.4000	0.3000
D-ZB	Time:	5.3137	69.539	139.75	172.15	150.34
	Vol.:	0.3001	0.5011	0.3012	0.3002	0.3021
D-CZ	Time:	0.7535	4.0616	3.7081	4.1103	4.3882
	Vol.:	0.3022	0.4001	0.4002	0.4011	0.4000

known reference points. Furthermore, $v_{1,k} = 0.02\rho_{y_1,k} - 0.01$, $v_{2,k} = 0.03\rho_{y_2,k} - 0.01$, $v_{3,k} = 0.03\rho_{y_3,k} - 0.02$, $v_{4,k} = 0.05\rho_{y_4,k} - 0.03$ and $\rho_{y_k,k} \in [0, 1]$ $(k = 1, 2, 3, 4)$.

Figure 3 illustrates the state estimation results when applying the methods i)–iv). As can be observed, the sets are fairly close to each other, with the V-H approach once more performing a little better than all other methods. Table III shows that RSRR and D-CZ have the lowest computation time, followed by the V-H approach. As expected, when the system dimension increases, the number of vertices when using the V-H approach also increases, resulting in higher average computation times, although they are still substantially lower than when using the D-ZB approach. Further, the volumes of the set estimates using all methods are comparable to each other. In contrast to Example I, we did not include the results from combining all methods (COMB), since they are identical to the ones from the V-H method.

VIII. CONCLUSION

Novel polytope-valued algorithms using direct V- and H-representations were proposed in this letter for state estimation in bounded-error nonlinear discrete-time systems subject to nonlinear observation/constraint functions. We adopted the commonly used two-step propagation and update strategy, where the propagated set estimates are obtained by computing a polytopic enclosure to the true range of the nonlinear vector field/system dynamics and the updated set estimates are computed by intersecting the predicted set with the set of states that are compatible with the observations/constraints. Our method relied on a novel approach to bound/enclose/outer-approximate the set-product of an interval matrix and a polytope. Further, sufficient conditions for the stability of the set-valued estimates were provided. Finally, the computational complexity of the proposed approach was studied, and its effectiveness was demonstrated by comparing the average volumes and computation times of the resulting sets with the ones returned by existing techniques in the literature.

REFERENCES

[1] M. A. Dahleh and J. B. Pearson, "ℓ_1-optimal feedback controllers for MIMO discrete-time systems," *IEEE Trans. Autom. Control*, vol. 32, no. 4, pp. 314–322, Apr. 1987.

[2] L. Jaulin, "A nonlinear set membership approach for the localization and map building of underwater robots," *IEEE Trans. Robot.*, vol. 25, no. 1, pp. 88–98, Feb. 2009.

[3] C. Combastel, Q. Zhang, and A. Lalami, "Fault diagnosis based on the enclosure of parameters estimated with an adaptive observer," *IFAC Proc. Vol.*, vol. 41, no. 2, pp. 7314–7319, 2008.

[4] B. S. Rego, G. V. Raffo, J. K. Scott, and D. M. Raimondo, "Guaranteed methods based on constrained zonotopes for set-valued state estimation of nonlinear discrete-time systems," *Automatica*, vol. 111, Jan. 2020, Art. no. 108614.

[5] M. Althoff and J. J. Rath, "Comparison of guaranteed state estimators for linear time-invariant systems," *Automatica*, vol. 130, Aug. 2021, Art. no. 109662.

[6] A. M. Tahir and B. Açıkmeşe, "Synthesis of interval observers for bounded Jacobian nonlinear discrete-time systems," *IEEE Contr. Syst. Lett.*, vol. 6, pp. 764–769, 2021.

[7] D. Efimov, T. Raïssi, S. Chebotarev, and A. Zolghadri, "Interval state observer for nonlinear time varying systems," *Automatica*, vol. 49, no. 1, pp. 200–205, 2013.

[8] M. Khajenejad and S. Z. Yong, "Simultaneous input and state set-valued $\mathcal{H}_\infty$-observers for linear parameter-varying systems," in *Proc. Amer. Control Conf. (ACC)*, 2019, pp. 4521–4526.

[9] M. Khajenejad and S. Z. Yong, "Simultaneous mode, in put and state set-valued observers with applications to resilient estimation against sparse attacks," in *Proc. Conf. Decis. Control (CDC)*, Nice, France, 2019, pp. 1544–1550.

[10] J. Wan, S. Sharma, and R. Sutton, "Guaranteed state estimation for nonlinear discrete-time systems via indirectly implemented polytopic set computation," *IEEE Trans. Autom. Control*, vol. 63, no. 12, pp. 4317–4322, Dec. 2018.

[11] C. Combastel, "Merging Kalman filtering and zonotopic state bounding for robust fault detection under noisy environment," *IFAC-PapersOnLine*, vol. 48, no. 21, pp. 289–295, 2015.

[12] T. Alamo, J. M. Bravo, M. J. Redondo, and E. F. Camacho, "A set-membership state estimation algorithm based on DC programming," *Automatica*, vol. 44, no. 1, pp. 216–224, 2008.

[13] J. K. Scott, D. M. Raimondo, G. R. Marseglia, and R. D. Braatz, "Constrained zonotopes: A new tool for set-based estimation and fault detection," *Automatica*, vol. 69, pp. 126–136, Jul. 2016.

[14] M. Althoff and B. H. Krogh, "Zonotope bundles for the efficient computation of reachable sets," in *Proc. IEEE Conf. Decis. Control Eur. Control Conf.*, Orlando, FL, USA, 2011, pp. 6814–6821.

[15] B. Rego, J. K. Scott, D. M. Raimondo, and G. V. Raffo, "Set-valued state estimation of nonlinear discrete-time systems with nonlinear invariants based on constrained zonotopes," *Automatica*, vol. 129, Jul. 2021, Art. no. 109638.

[16] M. Khajenejad, F. Shoaib, and S. Z. Yong, "Guaranteed state estimation via indirect polytopic set computation for nonlinear discrete-time systems," in *Proc. IEEE Conf. Decis. Control (CDC)*, 2021, pp. 6167–6174.

[17] M. Khajenejad and S. Z. Yong, "Tight remainder-form decomposition functions with applications to constrained reachability and guaranteed state estimation," 2021, *arXiv:2103.08638*.

[18] M. Althoff. *CORA 2020 Manual*. [Online]. Available: https://tumcps.github.io/CORA/data/Cora2020Manual.pdf (Accessed: Oct. 29, 2020).

[19] W. Kühn, "Rigorously computed orbits of dynamical systems without the wrapping effect," *Computing*, vol. 61, no. 1, pp. 47–67, 1998.

[20] Y. Yang, "A facet enumeration algorithm for convex polytopes," 2021, *arXiv:1909.11843*.

[21] B. Chen and G. Hu, "Nonlinear state estimation under bounded noises," *Automatica*, vol. 98, pp. 159–168, Dec. 2018.